



HAL
open science

Recent results on carrier selective three terminal perovskite on silicon-IBC tandem solar cells

J.P. Connolly, Koffi Ahanogbe, Jean-Paul P Kleider, J Alvarez, Hiroyuki Kanda, M K Nazeeruddin, Valentin Mihailetschi, Philippe Baranek, Malte Vogt, R Santbergen, et al.

► To cite this version:

J.P. Connolly, Koffi Ahanogbe, Jean-Paul P Kleider, J Alvarez, Hiroyuki Kanda, et al.. Recent results on carrier selective three terminal perovskite on silicon-IBC tandem solar cells. 37th European Photovoltaic Solar Energy Conference and Exhibition (EU PVSEC 2020), Sep 2020, Lisbon, Portugal. hal-02943627

HAL Id: hal-02943627

<https://hal.science/hal-02943627v1>

Submitted on 20 Sep 2020

HAL is a multi-disciplinary open access archive for the deposit and dissemination of scientific research documents, whether they are published or not. The documents may come from teaching and research institutions in France or abroad, or from public or private research centers.

L'archive ouverte pluridisciplinaire **HAL**, est destinée au dépôt et à la diffusion de documents scientifiques de niveau recherche, publiés ou non, émanant des établissements d'enseignement et de recherche français ou étrangers, des laboratoires publics ou privés.

RECENT RESULTS ON CARRIER SELECTIVE THREE TERMINAL PEROVSKITE ON SILICON-IBC TANDEM SOLAR CELLS

J.P. Connolly^{1a}, K. Ahanobge¹, J.P. Kleider¹, J. Alvarez¹, Hiroyuki Kanda², M.K. Nazeeruddin², V. Mihailetschi³, P. Baranek^{4,5}, Malte Vogt⁶, R. Santbergen⁶, O. Isabella⁶

¹ GeePs, LGEP, UMR CNRS 8507, Supelec, Université Pierre et Marie Curie, Université Paris-sud, 11 rue Joliot-Curie, 91192 Gif-sur-Yvette, France

² Group for Molecular Engineering of Functional Materials, Department of Chemistry and Chemical Engineering, Swiss Federal Institute of Technology, CH-1951 Sion, Switzerland

³ ISC Konstanz e.V., Rudolf-Diesel-Straße 15, Konstanz 78467, Germany

⁴ EDF R&D, Dept. EFESE, EDF Lab Paris-Saclay, 7 boulevard Gaspard Monge, 91120 Palaiseau, France

⁵ IPVF, 30 route Départementale 128, 91120 Palaiseau, France

⁶ Delft University of Technology, PVMD Group, Mekelweg 4, 2628 CD Delft, The Netherlands

ABSTRACT: The most successful high efficiency design, and one of the oldest, is the multi-junction solar cell. There are a range of multijunction solar cell terminal configurations, the specificities of which are reviewed, concluding with noting the increased attention being given to three terminal designs. This introduces a new device design which is the Three Terminal Selective Band Offset Barrier tandem solar cell. The physical operation of this new device is examined, and embodiments in prototype materials relying on materials properties from the literature. We present projected performance evaluated by two dimensional numerical modelling. Identifying shortcomings on two fronts of materials and optical properties of the multilayer stack, we describe theoretical progress in optimising these properties via ab initio materials modelling and combined ray and wave optics. This theoretical context introduces the experimental results obtained in the first year of the project. This consists of successful integration of the selective band offset barrier on a suitably modified IBC structure using prototype materials previously reported. This paper thereby presents detailed analysis of the three terminal selective band offset barrier tandem solar cell, and announces the first experimentally fabricated three terminal selective band offset barrier solar cells, together with preliminary conclusions of experimental characterisation which is underway.

Keywords: Multijunction ; Silicon ; Perovskite ; High efficiency ; Novel device

Author for correspondence : james.connolly@geeeps.centralesupelec.fr

1 INTRODUCTION

1.1 Multijunction terminal designs

Multijunction cells were the first high efficiency solar cell concept proposed, and resulted directly from the ideal Shockley radiative limit model which stated that what can absorb must emit according to the generalised Planck radiation law [1]. They have led to efficiencies in the region of 40% which are far above other designs to date [2].

This paper briefly reviews the field of multijunction terminal designs. This introduces recent progress on the recently patented [3] Three Terminal selective Band Offset Barrier Tandem solar cell (3T-SBOB) [4]. This has been previously introduced at EUPVSEC [5] in the context of the BOBTANDEM H2020 project in the Solar-ERANET programme [6].

1.2 Two terminal

Two terminal designs (fig. 1a) consist of cells connected by a tunnel junction. This design is attractive from a conceptual viewpoint presenting a single device with simple interconnections for module.

A first constraint is the compatible growth of lower and higher bandgap solar cell materials, which for best material quality requires compatible atomic lattices. Some advanced solutions such as strain-balancing or metamorphic growth techniques have achieved excellent results, but nevertheless this is an additional roadblock.

A second constraint for 2T structures is the constraint of series current continuity across all subcells. These must therefore yield equal photocurrents at their respective maximum power points in order to reach maximum

efficiency. In addition the tunnel junction is a component introducing manufacturing constraints on process temperature, and furthermore some voltage loss and some free carrier loss, and finally potential optical transmission issues.

This design is nevertheless the most efficient to date, since these issues can be addressed, at some cost in final system cost, as a consequence of which these devices are not yet widely implemented in terrestrial applications where cost is a premium.

1.2 Four terminal

Four terminal designs (fig. 1b) consist at their simplest of mechanically stacking. This consists of placing a high bandgap cell directly above a lower bandgap cell. Since this is generally inefficient due to optical transmission losses, four terminal devices are optimally designed with optical matching layers, at some cost in optical transmission, which may however be designed within acceptable limits.

In addition, 4T structures require careful alignment of contact grids (fig. 1b) or equal geometry naturally. This further requires optimisation of contacting schemes for three layers (top cell both contacts, and bottom cell top contact) which may limit optimum design for each cell. More importantly, this can only yield minimal shading if the cell follows incident sunlight with dual axis tracking. Any deviation will cause the grids to move out of alignment.

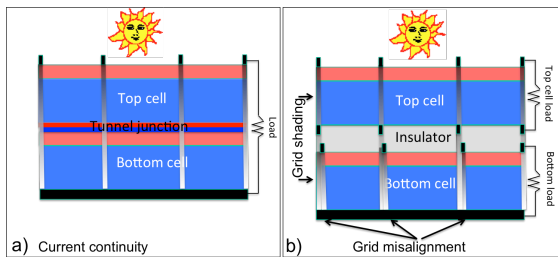


Figure 1: Schematic two terminal tandem (a) showing top grid shading, top cell and tunnel junction, and four terminal cell design showing the effect of possible grid misalignment.

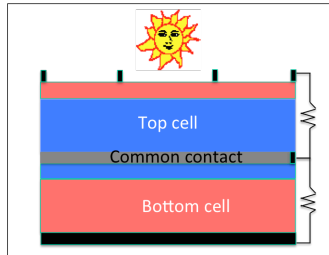


Figure 2: Schematic three terminal design where subcells are connected by a conduction layer corresponding to the joint third terminal.

1.2 Three terminal

Figure 3 introduces the three terminal (3T) design which has been gaining interest in recent years. This system is functionally similar to the 4T device where one short-circuits a common terminal. This common terminal corresponds to a common conducting layer connecting top and bottom rear and front contact layers.

This design can resolve issues of the 2T structure by eliminating lattice matching requirements, if top and bottom cells can be grown independently and connected by a non-crystalline conduction layer.

This does however leave this device sensitive to the optical and electrical properties of the transverse conduction layer which must carry the current of both top and bottom sub-cells. This leads to challenges in maintaining high conductivity to avoid resistance losses, while maintaining high optical transmission despite the presence of free carrier absorption in this conducting layer.

Worth mentioning is the bipolar transistor 3T solar cell proposed by Marti et al. [7]. This is a structure with elements reminiscent of transistors as the name suggests, with a common base sandwiched between high and low gap collector and emitter layers of opposite doping to the base.

1.2 Three Terminal Band Offset Barrier Tandems

This succinct review of existing terminal designs introduces the 3 Terminal-Selective Band Offset Barrier (3T-SBOB) tandem solar cell. This is reminiscent of the 3T solar cell with the major difference that the bottom subcell is an interdigitated back contact solar cell [8] no electrical contact is required between the cells.

The novelty of this 3T-SBOB design lies in the independent operation of two monolithically fabricated cells. This means that the two subcells have independent operating voltages and can operate at maximum power points determined by their respective bandgaps.

The design therefore delivers tandem efficiencies equal to 3T or 4T designs, but without the constraints 3T and 4T designs introduced previously.

The SBOB operation has some interesting precedents. The first is the very similar three terminal IBC tandem proposed by Nagashima [9]. The physical operation of this device is similar to the 3T-SBOB except that carrier selection is provided by doping contrast which produces barriers to carrier diffusion, in place of selective band offset barriers. The concept was demonstrated but the significantly lower selectivity of doping contrast is a limiting feature of this design.

The second is the Bariode [10]. This is an infra-red sensing device able to operate at higher temperatures due to a band-offset barrier inhibiting flow of one carrier, and reducing noise in low bandgap detectors. This Bariode detector which is in industrial production coincidentally demonstrates the principle of the concept at the heart of the 3T-SBOB.

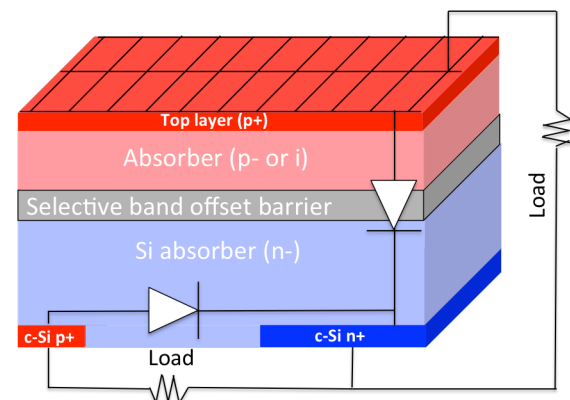


Figure 3: Schematic of the 3 Terminal-Selective Band Offset Barrier (3T-SBOB) tandem solar cell. Top and bottom cells are connected by a band offset barrier in one band which conducts only one carrier. The bottom cell is an interdigitated back contact cell and therefore currently limited to silicon.

Concluding this introduction we note one further point already reported previously [6] which is that the radiative efficiency contours of 2T and 3 or 4T show the broader optimum for 3 or 4T designs. This corresponds to the much lower sensitivity of these structures to the bandgap of top and bottom cells, which is to be expected given the elimination of the series current constraint.

The efficiency of 3T design is therefore much less sensitive to the bandgap of top and bottom cells, allowing consideration of a wide range of subcell materials.

2 SBOB OPERATING PRINCIPLES

2.1 Theory

The modelling of the 3T-SBOB has been implemented with numerical modelling using Silvaco software tools (ATLAS, ATHENA) [11] and details are not described in detail here.

We note only that a two dimensional approach is required in principle, given the two dimensional current flow in the IBC subcell, and that the modelling includes optical phase and therefore thin film effects and interference, via

the transfer matrix methodology.

For completeness the operating principles are repeated [6] for the schematic band structure shown in figure 4. This shows an n-type IBC in contact with selective band offset barrier (SBOB). The SBOB prevents the transport of one type of carrier, in this case holes, since the offset is in the valence band.

The other carrier (electrons) faces no such barrier since there is no band offset in the conduction band (because of the design principle “constant electron affinities” across the interface between top and bottom cells).

Since holes cannot cross the barrier, their distributions on either side are independent : No thermalisation occurs from the higher bandgap top cell to the lower bandgap IBC, and independent hole Fermi levels form.

Since electrons can cross without impediment, their population equilibrates, and they share a common Fermi level across the structure.

This produces quasi-Fermi level separations in top and bottom cells which are independent, and determined by the bandgap of the materials in each.

As a result, both cells operate independently, and the structure yields tandem efficiencies.

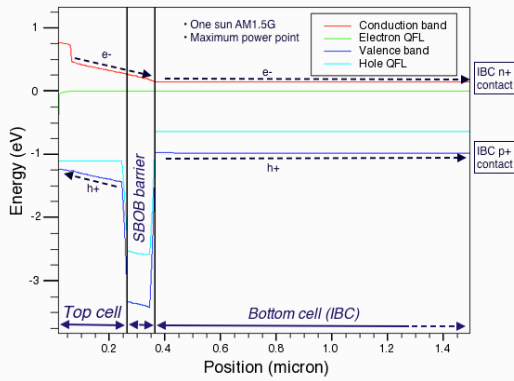


Figure 4: 3T-SBOB band structure and operating principle under illumination for a n-type IBC. For this polarity, top cell photogenerated electrons are collected in the bottom cell. Top cell holes are collected by the hole transport later at the front of the top cell. The IBC operation is unchanged, with electrons collected at the n+ layer and cathode, and holes at the front surface and back contact anodes. The result is independent carrier populations of holes in both cells, and independent quasi-Fermi level separations, and minimal thermalisation loss, yielding 3T tandem solar cell efficiencies without a contact needed between the top and bottom cells.

2.2 First stage prototypes

In the first stages of this work, materials evaluated included III-V materials which are mentioned to give a perspective of the conception of the work and an indication of identification fo real materials.

Figure 5 shows the band structure for a AlInP SBOB and al AlGaAs absorber. In this case (details of compositions and materials parameters which are well known are not indicated for brevity) the AlInP affinity is slightly greater than the AlGaAs, giving a very slight barrier of about 10meV for electron diffusion. Since this is lower than the thermal voltage, this has minimal influence on electron collection of top cell electrons at the cathode of the bottom cell. On the other hand, we note a significant conduction drop from the AlInP SBOB to the IBC, due to

the lower affinity of the latter. This is a significant shortcoming, since such a bias drop translates directly as a voltage loss for top cell operation.

Nevertheless, the somewhat idealised (no interface defects are present in particular) efficiencies shown in figure 6 reach about 30%.

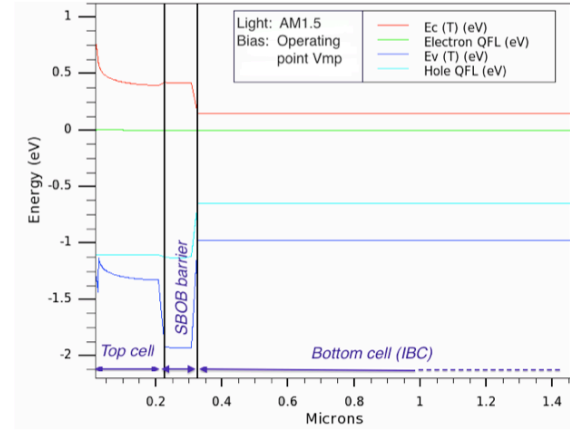


Figure 5: Numerical calculation of the band structure of a 3T-SBOB prototype featuring for the top cell a AlGaAs absorber and AlInP emitter. The band structure is shown at the maximum power point.

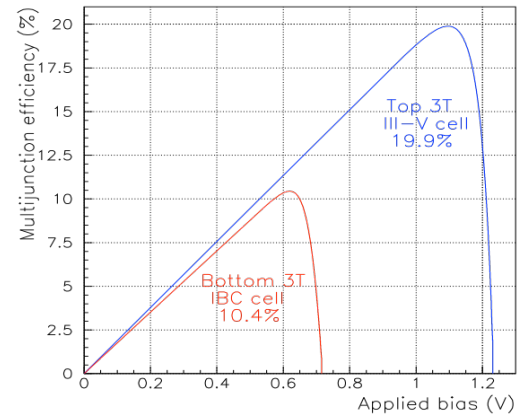


Figure 6: Numerical modelling of the III-V (AlGaAs / AlInP / IBC) 3T-SBOB showing an efficiency reaching over 30%.

2.3 The BOBTandem device : Perovskites on silicon

Extending the modelling to perovskites on silicon IBCs has similarly followed an initial idealised description using approximate materials parameters which produced efficiencies in the region of 35% (details not shown here).

A more thorough investigation of materials parameters has included data from the literature, starting with the extensive work of Minemoto [12] who developed early physical models and materials parameter databases, supplemented by further work by [13, 14]. This has been complemented by measured optical materials parameters by partners at CEA-LITEN for MAPI, SnO₂, and PTAA used in this work.

Figure 7 shows simply the layer configuration of the PSC top cell. The IBC cell is a $\approx 160\mu\text{m}$ ZEBRA cell manufactured by ISC-Konstanz. Not shown are the back

interdigitated back contacts.

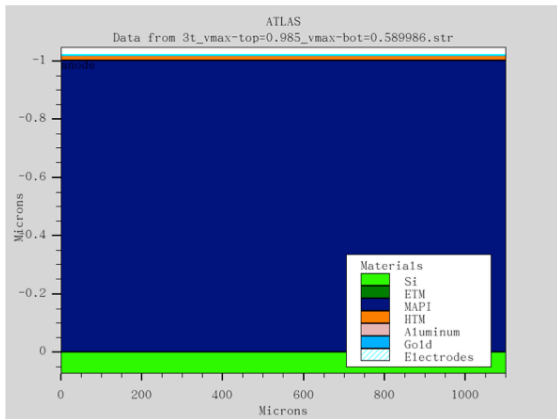


Figure 7: Silvaco schematic of the PSC cell. Not shown is the full structure dominated by the homogeneous 160 μm IBC cell, nor the ISC-Konstanz ZEBRA cell back contact configuration.

To illustrate the working cell, figure 8 shows the band structure at operating point, showing a clear difference in quasi-Fermi level separation. An interesting discussion is possible examining the band profiles as a function of independent bias for each junction. Though beyond the scope of this paper, such an analysis shows the independent operation of each subcell, one cell for example being maintained at short circuit while the other is varied from short circuit to the open circuit condition.

The current flows over the entire structure are shown in figure 9a, with a zoom on the perovskite solar cell illustrated in figure 9b, and on the IBC back contacts in figure 9c which are not the experimental ones for illustrative purposes.

The principal observations from these graphs is the circulation of current from bottom to top cell as expected, and current circulating from IBC anode to cathode, as expected.

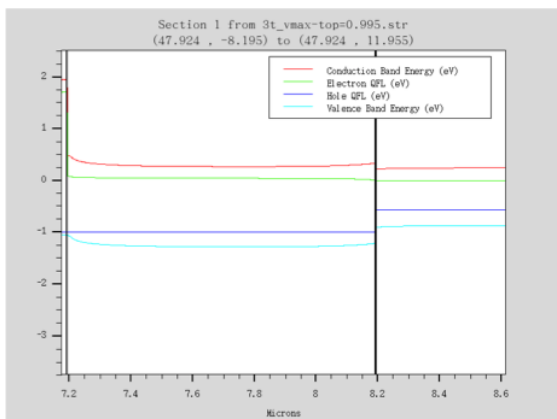


Figure 8 3T-SBOB Band structure at operating point.

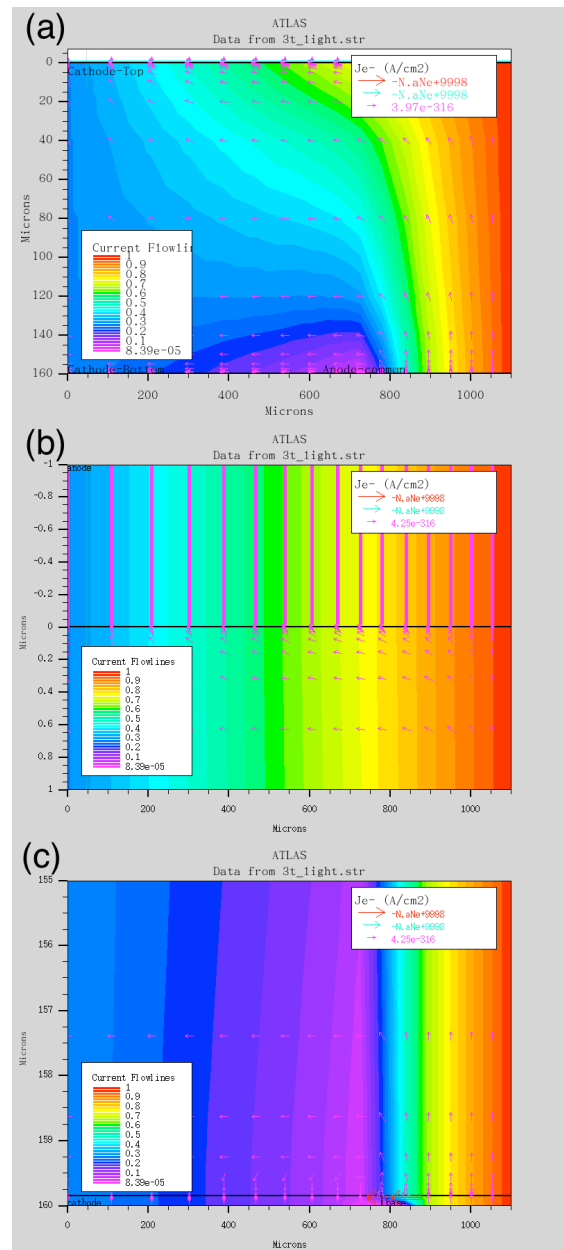


Figure 9 Current flows (a) over the entire cell (b) Over the PSC and IBC and (c) over the IBC contacts (contacts not to scale).

The performance of the cell is summarised in figure 10, though detailed results examining current voltage curves for top and bottom cells are not included here in order to focus on the main features of these studies.

The Si solar cell efficiency is markedly low. This is due to the low bandgap of the MAPI considered in these studies.

The PSC efficiency on the other hand is very high. It is of the order of very good experimental results obtained in this system by the team at EPFL, and therefore in principle not unrealistic, but however is a significant over-estimate in the context of early prototypes of PSCs grown on Si – IBCs.

These points are confirmed by examining the quantum efficiency (fig. 11). This shows a satisfactory PSC

response, and an EQE nearly reaching 100%, due to the presence of a single layer AR coat.

The Si-IBC however is crippled by the relatively low bandgap of the PSC. Although referring to radiative efficiency contours [6] shows that such a low PSC gap can reach 40.5% in the radiative limit, whereas the ideal combination is a PSC gap of 1.85eV for a Si lower gap of 1.12eV which reaches 42% (fig 12).

IBC bottom cell		PSC top cell	
Vmp	= 0.59V	Vmp	= 0.96V
Voc	= 0.68V	Voc	= 1.13V
Jsc	= 10.08mA/cm2	Jsc	= 26.45mA/cm2
Efficiency	= 5.63%	Efficiency	= 23.7%

Figure 10 Figures of merit for the simulated 3T-SBOB, giving an overall efficiency of 29.33% under AM1.5G.

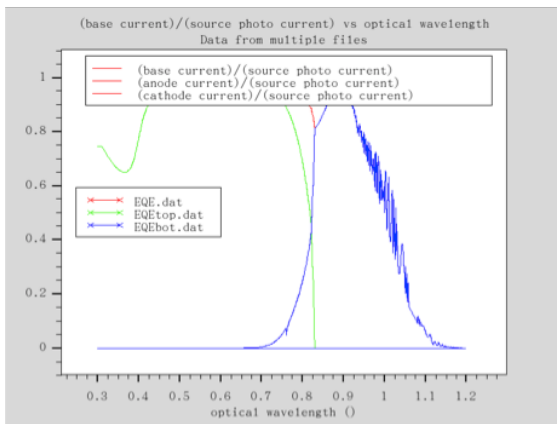


Figure 11 External quantum efficiency showing an efficient PSC but an IBC suffering from low absorption and from interference effects due to the sub-optimal optical stack, particularly the PSC layers.

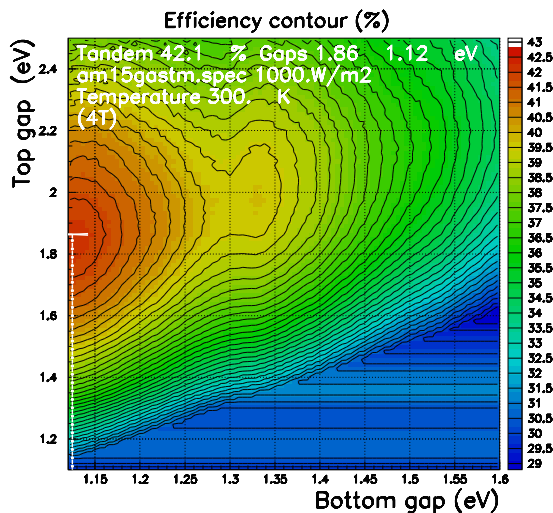


Figure 12 Radiative efficiency showing the maximum efficiency for a Si- bottom cell.

3 LATE NEWS – FIRST FABRICATION

Slightly ahead of schedule, the first 3T-SBOB samples were fabricated in August 2020. Since this is work in progress a few weeks old, it is beyond the scope of this paper to enter into details of fabrication and composition of the PSC device in particular.

It can be said that preliminary devices featured front surface metal contacting on the PSC, thereby limiting light transmission and leading to low efficiencies for both subcells. Nevertheless, separate characterisation of both subcells showed working photovoltaic cells. A second set of cells with improved front contacting has significantly increased efficiencies.

While these will be published in detail shortly, we can announce at this conference that the first 3T-SBOB devices have been fabricated and show preliminary confirmation of the independent operation as expected from the numerical modelling.

4 NEXT STEPS

Following the analysis laid out in this contribution, two theoretical elements come to the fore.

The first is the theoretical optimisation of materials along lines we do not have space to go in to here but which is underlined by the sub-optimum materials we have presented. The approach is however based on evaluation of existing materials, and in using ab initio modelling to evaluate more optimum materials and compositions. This work includes evaluation of growth conditions and interface properties and is carried out by the EDF partner of the project.

The second is the optimisation of the optical properties of the layer stack making up the 3T-SBOB. The current numerical modelling shows shortcomings on two fronts : One is the presence of interference effects due to sub-optimal choice of refractive indices, and layer thicknesses. This feeds back to the materials modelling activity which can propose materials with more suitable optical refractive indices in the highly tunable perovskite family of materials, and beyond. The optical modelling is being studied by the TUD group [15].

5 CONCLUSIONS

The aim of this paper has been to update the current status of the BOBTandem project investigating a new device, the operation of which has not yet been confirmed experimentally.

The background to this new device has been sketched by giving an overview of contact terminal approaches for multijunction solar cells. The physical operating principles have been put in context by mentioning concepts with related ideas.

The physical operation of the structure has been sketched in different materials systems, concluding with a model of the main structure being considered, which is a perovskite PSC on a silicon IBC. This has identified shortcomings in both the structure and in the modelling.

Finally, we announce the most important progress, which is the first fabrication of the novel 3T-SBOB device. Experimental results will follow shortly and will be reported on the project website [5].

Acknowledgements : The authors acknowledge the support of the H2020 Solar-ERANET program, and the ANR French national funding agency, which have funded the Solar-ERANET project BOBTANDEM (2019-2022).

References

- [1] W. Shockley, H. J. Queisser, "Detailed balance limit of efficiency of p-n junction solar cells" *Journal of Applied Physics*, 32, 510 (1961).
<https://doi.org/10.1063/1.1736034>
- [2] Martin A. Green et al., *Solar cell efficiency tables (version 56)*, Progress in Photovoltaics, Volume 28, Issue 7, July 2020.
- [3] Z. Djebbour, W. El-Huni, A. Migan and J-P. Kleider, Patent WO 2017/093695
- [4] J.-P. Kleider, Z. Djebbour, A. Migan-Dubois, W. El-Huni, C. Leon, M.E. Gueunier-Farret, J.P. Connolly, "Three-Terminal Tandem Solar Cells Combining Bottom Interdigitated Back Contact and Top Heterojunction Subcells: A New Architecture for High Power Conversion Efficiency", 35th EU PVSEC, 4 to 28 September 2018, Brussels,
<https://doi.org/10.4229/35thEUPVSEC20182018-1AO.2.4>
- [5] H2020 (Solar-ERANET) project BOBTANDEM
Web: <https://bobtandem.wordpress.com/>
Twitter: <https://twitter.com/BobTandem>
- [6] J.P. Connolly et al., "Designing Carrier Selective Perovskite on Silicon 3T Tandems", 36th EU PVSEC,
<https://doi.org/10.4229/EUPVSEC20192019-3BV.2.60>
- [7] A. Martí, A. Luque, "Three-terminal heterojunction bipolar transistor solar cell for high-efficiency photovoltaic conversion", *Nature Communications*, 2015
<http://dx.doi.org/10.1038/ncomms7902>
- [8] A. Halm, V.D. Mihailetschi, et al., "The Zebra Cell Concept - Large Area n-Type Interdigitated Back Contact Solar Cells and One-Cell Modules Fabricated Using Standard Industrial Processing Equipment", 27th EU-PVSEC (2012)
<http://doi.org/10.4229/27thEUPVSEC2012-2AO.2.1>
- [9] Tomonori Nagashima et al, 28th IEEE-PVSEC, Anchorage (2000),
<http://dx.doi.org/10.1109/PVSC.2000.916102>
- [10] Philip Klipstein et al., "High operating temperature X_{Bn}-InAsSb barrier detectors", *Proc. SPIE* 8268, Quantum Sensing and Nanophotonic Devices IX, 82680U (2012); <http://dx.doi.org/10.1117/12.910174>
- [11] Z. Djebbour et al., "Bandgap engineered smart three-terminal solar cell: New perspectives towards very high efficiencies in the silicon world", *Prog Photovolt Res Appl.* 27, 4 pp. 306-315 (2019);
<http://dx.doi.org/10.1002/pip.3096>
- [12] Takashi Minemoto, Masashi, Murata, "Impact of work function of back contact of perovskite solar cells without hole transport material analyzed by device simulation", *Current Applied Physics* Volume 14, Issue 11, November 2014, Pages 1428-1433, <https://doi.org/10.1016/j.cap.2014.08.002>
- [13] Kai Tan *et al.*, "Controllable design of solid-state perovskite solar cells by SCAPS device simulation", *Solid-State Electronics*, Volume 126, December 2016, Pages 75-80,
<https://doi.org/10.1016/j.sse.2016.09.012>
- [14] Burschka, J., Pellet, N., Moon, S. et al. "Sequential deposition as a route to high-performance perovskite-sensitized solar cells". *Nature* 499, 316–319 (2013).
<https://doi.org/10.1038/nature12340>
- [15] R. Santbergen et al., *IEEE J. Photovolt.* 94 (2017) 919-926